第 30 卷 第 6 期 焊 接 学 报 Vol. 30 No. 6
2009 年 6 月 TRANSACTIONS OF THE CHINA WELDING INSTITUTION June 2009

超声焊接压电换能器的研制

齐海群， 单小彪， 谢 涛
（哈尔滨工业大学 机电工程学院，哈尔滨 150001）

齐海群

摘 要：基于变截面杆作一维纵向振动运动方程，在理论分析的基础上，根据四端网络传递方程和端面运动状态推导出了常用截面形状细杆在各种运动状态下边界条件和四端网络传递矩阵参数以及频率方程. 研究了适用于超声焊接的压电换能器的设计方法. 为说明设计方法，利用四端网络法对压电换能器和变幅杆进行了设计. 利用阻抗分析仪测量和分析了超声换能系统的谐振特性，并进行了系统的振动测试. 分析和测试结果验证了设计的正确性.

关键词：变截面杆；压电换能器；四端网络法；性能分析
中图分类号：TB55 文献标识码：A 文章编号：0253－360X(2009)06－0017－04

0 序 言

超声焊接是一种可点焊、连续焊等各种焊接工作方式的焊接方法，易于实现焊接的控制；结合时间短，结合部分不产生铸造组织缺陷；能在同种金属、不同种金属之间进行焊接，尤其适用于金属管材、箔片、细丝、微小器件等的特殊焊接[1]. 由于能连续焊、速度快、强度高、能耗低，因此倍受焊接生产企业的欢迎. 超声焊接装置由焊接头、发生器、换能器、变幅杆、调速电机、变频器、压缩机、汽缸等组成. 超声焊接的主要参数是频率、振幅、静压力及焊接时间，而决定频率和振幅的核心部件是换能器和变幅杆. 工艺研究表明，换能器的频率和振幅是影响焊接强度的主要参数，简洁、方便、可靠地设计换能系统是保证焊接质量的关键[2]. 文中以谐振频率 21 kHz，输出振幅 10 μm 以上的换能器和变幅杆设计为例，探讨一种新的超声换能系统的研制方法.

1 四端网络设计法

1.1 变截面细杆的一维纵振方程和四端网络法

在超声加工领域，常采用一种在压电陶瓷圆片两端面夹以金属块而组成的夹心式换能器. 在设计时为了简化分析夹心式换能器的振动状态，进行如下假设：换能器的总长度要和超声波长相比拟，换能器的直径必须小于超声波长. 在这一假设下，换能器的振动可以近似看成一个细长变截面细棒的纵向振动. 在换能器的各组成部件的连接面两侧位移和应力是连续的，因此对于夹心式换能器可以抽象成一个复合细杆振动的理想模型.

任意截面形状的均质细杆如图 1 所示，长为 L，横截面积为 $S(x)$，X 截面上的纵向位移为 ξ，则可得细杆纵向自由振动的运动方程为[3]

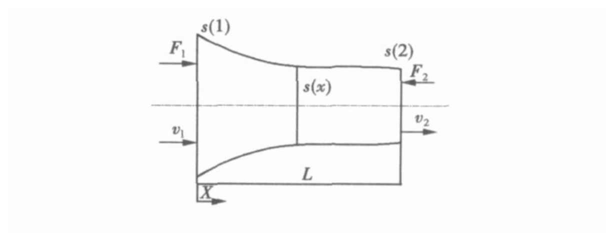

图 1 任意截面形状的均质细杆

Fig 1 Variable cross-section bar

$$c^2\left[S(x)\frac{\partial \xi}{\partial x}\frac{\partial \xi}{\partial x}\right]=S(x)\frac{a^2\xi}{\partial x^2} \quad (1)$$

若振子随之亦做简谐振动，即 $\xi=v=\mathrm{j}\omega\xi$，则式(1)可简化为

$$\frac{\partial^2 v}{\partial x^2}+\frac{1}{S(x)}\frac{\partial x(x)}{\partial x}\frac{\partial v}{\partial x}+k^2 v=0 \quad (2)$$

式中：k 为波数. 对式(2)做变换 $v=y/\sqrt{S}$，得

$$\frac{\partial^2 y}{\partial x^2}+k_1^2 y=0 \quad (3)$$

收稿日期：2008－01－04
基金项目：黑龙江省自然科学基金项目(E200614)

其中 $k_1^2=k^2-\frac{1}{S}\frac{\mathrm{d}^2\sqrt{S}}{\mathrm{d}x^2}$. 式(3)有简谐解 $y=A\sin(k_1x)+\cos(k_1x)$. 因此, 细杆的振动速度函数和力函数分别为

$$v(x)=\frac{1}{\sqrt{S}}[A\sin(k_1x)+\cos(k_1x)] \tag{4}$$

$$F(x)=\frac{yS(x)}{\mathrm{j}\omega}\frac{\partial v}{\partial x} \tag{5}$$

由细杆两端的边界条件:

$v\,|_{x=0}=v_1,\ v\,|_{x=L}=v_2$

$F\,|_{x=0}=-F_1,\ F\,|_{x=L}=-F_2$

可以得到细杆的机械运动方程组

$$\left.\begin{aligned}F_1&=\frac{\rho c}{2\mathrm{j}k}\frac{\partial S_1}{\partial x}v_1+\frac{\rho ck_1S_1}{\mathrm{j}k\tan(k_1L)}v_1-\frac{\rho ck_1\sqrt{S_1S_2}}{\mathrm{j}k\sin(k_1L)}v_2\\F_2&=\frac{\rho c}{2\mathrm{j}k}\frac{\partial S_2}{\partial x}v_2+\frac{\rho ck_1S_2}{\mathrm{j}k\tan(k_1L)}v_2-\frac{\rho ck_1\sqrt{S_1S_2}}{\mathrm{j}k\sin(k_1L)}v_1\end{aligned}\right\} \tag{6}$$

由式(6), 可得

$$\left.\begin{aligned}a_{11}&=\frac{(\partial S_1/\partial x)\sin(k_1L)+2k_1S_1\cos(k_1L)}{2k_1\sqrt{S_1S_2}}\\a_{12}&=-\frac{\mathrm{j}k\sin(k_1L)}{\rho ck_1\sqrt{S_1S_2}}\\F_2&=a_{21}v_1+a_{22}F_1\\a_{21}&=\frac{\rho ck_1\sqrt{S_1S_2}}{\mathrm{j}k\sin(k_1L)}-a_{11}\left(\frac{\rho ck_1S_2}{\mathrm{j}k\tan(k_1L)}-\frac{\rho c}{2\mathrm{j}k}\frac{\partial S_2}{\partial x}\right)\\a_{22}&=-a_{12}\left(\frac{\rho ck_1S_2}{\mathrm{j}k\tan(k_1L)}-\frac{\rho c}{2\mathrm{j}k}\frac{\partial S_2}{\partial x}\right)\end{aligned}\right\} \tag{7}$$

任意截面杆都可等效为一个四端网络如图 2 所示.

图 2　单一截面杆的等效四端网络

Fig 2　Four-terminal network of single bar

其传输方程为
$$\begin{bmatrix}v_2\\F_2\end{bmatrix}=\begin{bmatrix}a_{11}&a_{12}\\a_{21}&a_{22}\end{bmatrix}\begin{bmatrix}v_1\\F_1\end{bmatrix} \tag{8}$$

其中 $\begin{bmatrix}a_{11}&a_{12}\\a_{21}&a_{22}\end{bmatrix}$ 为传输矩阵.

当截面杆的两端自由振动时, 两端的位移最大, 此时的传输特性方程为

$$\begin{bmatrix}v_2\\0\end{bmatrix}=\begin{bmatrix}a_{11}&a_{12}\\a_{21}&a_{22}\end{bmatrix}\begin{bmatrix}v_1\\0\end{bmatrix} \tag{9}$$

此时的频率方程为 $a_{21}=0$, 两端的振动速度为 $v_2/v_1=a_{11}$.

同理, 当截面杆的前端自由振动, 后端被夹持时, 频率方程为 $a_{11}=0$; 当截面杆的前端被夹持、后端自由振动时, 频率方程为 $a_{22}=0$; 当截面杆的前后端都被夹持时, 频率方程为 $a_{12}=0$.

由上述 4 种情况就可以对任意截面杆的换能器或者变幅杆进行推导, 最终求得各自的频率方程和两端的振速比.

1.2　传输参数及多截面杆的四端网络求解法

超声振子一般由多个不同截面形状的杆件连接而成, 常用杆件的形状有等截面、圆锥形等形状.

对于超声加工用的换能器以及变幅杆, 常利用各种形状截面杆进行复合. 因此对于多截面杆的复合进行四端网络的研究是非常必要的, 如图 3 所示以两个截面杆进行四端网络的分析.

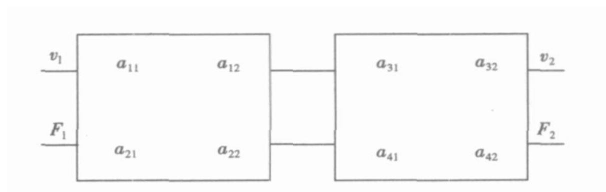

图 3　两截面杆的四端网络图

Fig. 3　Four-terminal network of two bar

其中: $\begin{bmatrix}a_{11}&a_{12}\\a_{21}&a_{22}\end{bmatrix}$ 为第一截面杆的四端网络传输矩阵; $\begin{bmatrix}a_{31}&a_{32}\\a_{41}&a_{42}\end{bmatrix}$ 为第二截面杆的四端网络传输矩阵; $\boldsymbol{A}=\begin{bmatrix}a_{31}&a_{32}\\a_{41}&a_{42}\end{bmatrix}\begin{bmatrix}a_{11}&a_{12}\\a_{21}&a_{22}\end{bmatrix}=\begin{bmatrix}b_{11}&b_{12}\\b_{21}&b_{22}\end{bmatrix}$ 为整体的传输矩阵; $b_{11}=a_{31}a_{11}+a_{32}a_{21}$; $b_{12}=a_{31}a_{12}+a_{32}a_{22}$; $b_{21}=a_{41}a_{11}+a_{42}a_{21}$; $b_{22}=a_{41}a_{12}+a_{42}a_{22}$. 根据前后端面的运动状态和连接状态, 即可确定整体的频率方程以及两端的振速比.

2　换能器和变幅杆设计

2.1　换能器设计

为了确定换能器的共振频率必须有换能器频率方程, 根据前面得出的一维振动速度和应力方程完全可以得出换能器的频率方程. 文中设计的夹心式换能器采用纵向复合结构如图 4 所示. 设计谐振频率为 21 kHz, 采用四分之一波长换能器振子和四分之一波长阶梯形变幅杆组成[4].

节面左端的四端网络传输方程为

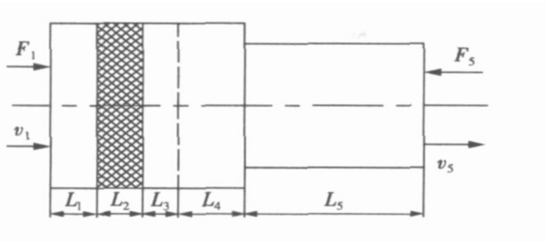

图 4　换能器结构简图

Fig. 4　Diagram of the transducer

$$\begin{bmatrix} v_3 \\ F_3 \end{bmatrix} = \begin{bmatrix} a_{11} & a_{12} \\ a_{21} & a_{22} \end{bmatrix} \begin{bmatrix} v_1 \\ F_1 \end{bmatrix} \tag{10}$$

其中根据节面左侧部分的运动状态及受力状况确定两端的参数 $v_3=0$, $F_1=0$. 传输矩阵为

$$\begin{bmatrix} a_{11} & a_{12} \\ a_{21} & a_{22} \end{bmatrix} = \begin{bmatrix} a^3_{11} & a^3_{12} \\ a^3_{21} & a^3_{22} \end{bmatrix} \begin{bmatrix} a^2_{11} & a^2_{12} \\ a^2_{21} & a^2_{22} \end{bmatrix} \begin{bmatrix} a^1_{11} & a^1_{12} \\ a^1_{21} & a^1_{22} \end{bmatrix} \tag{11}$$

将四端网络传输矩阵参数代入节面左侧即四分之一波长换能器的传输矩阵可得 $a_{11}=0$. 其谐振频率方程为

$$\frac{Z_1}{Z_3}\tan(k_2L_2)\tan(k_1L_1)+\frac{Z_1}{Z_3}\tan(k_1L_1)\tan(k_3L_3)+\frac{Z_2}{Z_3}\tan(k_3L_3)\tan(k_2L_2)=1 \tag{12}$$

对于节面右端即四分之一波长阶梯形变幅杆的四端网络传输方程为

$$\begin{bmatrix} v_5 \\ F_5 \end{bmatrix} = \begin{bmatrix} a_{11} & a_{12} \\ a_{21} & a_{22} \end{bmatrix} \begin{bmatrix} v_4 \\ F_4 \end{bmatrix} \tag{13}$$

其中根据节面左侧部分的运动状态及受力状况确定两端的参数 $v_4=0$, $F_5=0$. 传输矩阵为

$$\begin{bmatrix} a_{11} & a_{12} \\ a_{21} & a_{22} \end{bmatrix} \begin{bmatrix} a^5_{11} & a^5_{12} \\ a^5_{21} & a^5_{22} \end{bmatrix} \begin{bmatrix} a^4_{11} & a^4_{12} \\ a^4_{21} & a^4_{22} \end{bmatrix} \tag{14}$$

将四端网络传输矩阵参数代入节面左侧即四分之一波长换能器的传输矩阵可得 $a_{22}=0$. 其谐振频率方程为

$$\frac{Z_4}{Z_5}=\tan(k_4L_4)\tan(k_5L_5) \tag{15}$$

换能器所用材料涉及到 45 钢、压电陶瓷和硬铝合金. 查得三种材料的相关参数为 $\rho_1=7.8\times10^3$ kg/m^3, $\rho_2=7.5\times10^3$ kg/m^3, $\rho_3=2.7\times10^3$ kg/m^3, $c_1=$ 5 150 m/s, $c_2=$ 5 050 m/s, $c_3=$ 3 100 m/s. 如图 4 所示后端盖和压电陶瓷通过硬铝合金与换能器连接起来, 所以如果完全按照后端盖和压电陶瓷的材料属性来进行计算肯定存在很大误差, 所以采用等效面积法进行计算.

为与压电陶瓷配合, 在此取后端盖 $2D=$ 48.5 mm, 节面的厚度 $L_1=28$ mm, 压电陶瓷的厚度根据选取的陶瓷片的厚度确定为 $L_2=12$ mm, 将相关参数带入已知两个谐振频率方程得 $L_3=4$ mm, L_4 $=35$ mm, $L_5=44$ mm.

2.2　变幅杆设计

变幅杆的设计主要根据系统的频率、放大倍数以及焊头的形状等许多条件决定. 常见变幅杆的形状有阶梯形、圆锥形等几种[5]. 而复合变幅杆通常有变截面杆和等截面杆两部分组成, 为了获得较高的变速比同时根据加工条件的需要, 采用圆锥形变截面杆.

根据变幅杆的运动状态及受力状况确定两端的参数 $F_6=0$, $F_7=0$. 传输矩阵为

$$\begin{bmatrix} a_{11} & a_{12} \\ a_{21} & a_{22} \end{bmatrix} = \begin{bmatrix} a^7_{11} & a^7_{12} \\ a^7_{21} & a^7_{22} \end{bmatrix} \begin{bmatrix} a^6_{11} & a^6_{12} \\ a^6_{21} & a^6_{22} \end{bmatrix} \tag{16}$$

将四端网络传输矩阵参数代入节面左侧即四分之一波长变幅杆的传输矩阵可得 $a_{21}=0$, 其谐振频率方程为

$$\tan(k_7L_7)=\frac{(N-1)^2k_6L_6-[N(k_6L_6)^2-(N-1)^2]-(N-1)^2\tan(k_6L_6)}{k_6L_6[Nk_6L_6-(N-1)\tan(k_6L_6)]} \tag{17}$$

代入已知条件, 由谐振频率方程得 $L_6=40$ mm, $L_7=70$ mm. 根据变幅杆共振条件要求焊头的长度也必须满足半波长, 初步确定焊头的长度, 在动力学分析中再进行调整.

3　系统的阻抗分析和振动测试

3.1　阻抗分析

为了解换能器以及整个振动系统的阻抗特性, 获取其谐振频率, 采用 HP4294A 阻抗分析仪测量和分析超声换能系统的谐振特性, 其测量结果如图 5 所示. 由图可以清晰地看到换能器的谐振频率为 21.43 kHz, 其阻抗约为 668.501 Ω, 相角为 $-55.605\,4^\circ$. 由此可知, 超声换能系统的实际工作频率和设计频率 21 kHz 较为接近.

3.2　振动测试

为衡量超声换能系统的性能和工作状态, 采用工具显微镜和德国产 Polytec 扫描式激光测振仪对系统进行振动测试.

图 6 为施加超声前后变幅杆端面的比较图, 此时频率为 20.727 kHz, 测得端面的差值 $L=10$ mm, 计算得系统的振幅约为 17 μm.

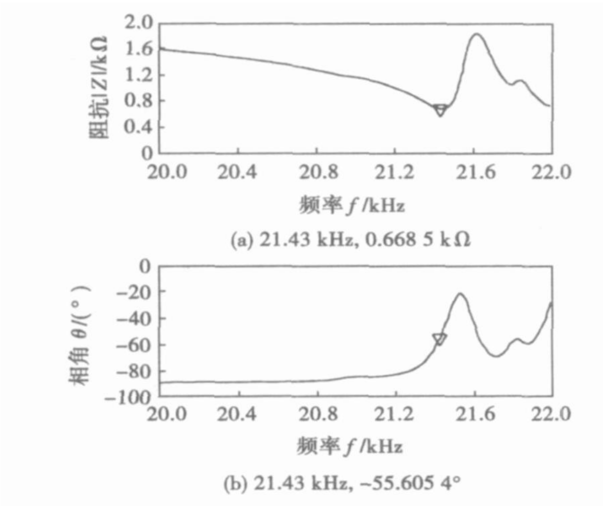

图 5 振换能器的阻抗特性曲线

Fig. 5 Impedance characteristics of transducer

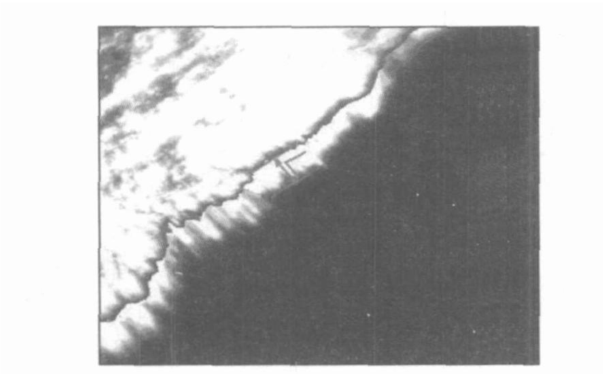

图 6 变幅杆端面轮廓图

Fig 6 Side-outline of transformer

图 7 为采用激光测试系统获得的施加超声时的变幅杆端面振动动画,此时测得系统的振动频率为 20.745 kHz.

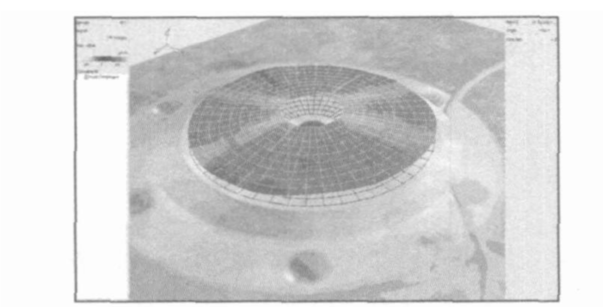

图 7 变幅杆端面振动动画

Fig. 7 Vibration-animation of transformer-side

4 结 论

(1) 对任意截面杆纵向自由振动的情况进行了分析,得出常用截面细杆的四端网络矩阵参数并推导出几种常见运动状态的频率方程.

(2) 根据压电换能器设计的基本原理,设计了适合超声焊接的超声换能系统.

(3) 对超声换能系统进行了阻抗分析和振动测试,结果表明系统的设计频率和工作频率结果接近,超声换能系统性能良好满足设计要求.

参考文献:

[1] 陈思忠, 郑伟成, 都文华, 等. 铝塑复合管的超声金属焊接[J]. 应用声学, 2000, 19(4): 1-4.

Chen Sizhong, Zheng Weicheng, Du Wenhua, *et al*. Ultrasonic metal welding of aluminum-plastics composite tube[J]. Applied Acoustics, 2000, 19(4): 1-4.

[2] 王福军, 赵兴玉, 张大卫, 等. 热超声键合压电换能器的动力学特性[J]. 焊接学报, 2008, 29(10): 69-72.

Wang Fujun, Zhao Xingyu, Zhang Dawei, *et al*. Dynamic characteristics study of piezoelectric transducer for thermosonic bonding[J]. Transactioins of the China Welding Institution, 2008, 29(10): 69-72.

[3] 林仲茂. 超声变幅杆的原理和设计[M]. 北京: 科学出版社, 1987.

[4] 朱 武, 张佳民. 超声振动系统设计及性能分析[J]. 上海电力学院学报, 2004, 20(3): 47-50.

Zhuw Wu, Zhang Jiamin. Designing and performance analysis of ultrasonic vibration system[J]. Journal of Shanghai University of Electric Power, 2004, 20(3): 47-50.

[5] 林书玉. 夹心式功率超声压电陶瓷换能器的工程设计[J]. 声学技术, 2006, 25(2): 160-164.

Lin Shuyu. Design of sandwich piezoelectric ceramic ultrasonic transducer[J]. Technical Acoustics, 2006, 25(2): 160-164.

作者简介: 齐海群, 男, 1965 年出生, 博士研究生, 教授. 主要从事仿真机构、超声加工方面的科研和教学工作. 发表论文近 20 篇.

Email: qihaiqun8@126.com

MAIN TOPICS, ABSTRACTS & KEY WORDS

Non-destructive evaluation of FSW tensile property GANG Tie, ZHAO Xuemei, LIN Sanbao, LUAN Yilin (State Key Laboratory of Advanced Welding Production Technology, Harbin Institute of Technology, Harbin 150001, China). p 1—4

Abstract: Elastic module, microstructure of materials and corresponding mechanical properties can be characterized by ultrasonic methods, especially, the microstructure, a crucial factor of mechanical properties, correlating with ultrasonic attenuation obviously. In the present research, a focusing angle beam immersion system was adopted to receive the transmission wave which represents to penetrated attenuation caused by the different microstructure of friction stir welding (FSW) joints, and the feature of FSW joints had been extracted from C-scan images for non-destructive evaluation of the tensile properties of welds. A desirable correlation between the calculating and testing results of ultimate tensile strength was presented, which indicates the feasibility of predicting mechanical properties of FSW joints by ultrasonic methods.

Key words: non-destructive evaluation; ultimate tensile strength; friction stir welding; C-scan

Influence of dynamic electromagnetic force on stability of short-circuiting transfer in GMAW HE Jianping[1], WU Yixiong[2], JIAO Fujie[1] (1. School of Materials Engineering, Shanghai University of Engineering Science, Shanghai 201260, China; 2. Laser Manufacture and Research Center, Shanghai Jiaotong University, Shanghai 200240, China). p 5—8

Abstract: Problems about dynamic force equilibrium on liquid droplet during arc period of short-circuiting transfer are theoretically approached. Dynamic electro-magnetic force and its influence on the stability of short-circuiting transfer during arc period of short-circuiting transfer are mainly discussed. The results show that the dynamic change of electro-magnetic force on droplet relates to the variations of droplet size, arc root position and welding current. If dynamic force equilibrium on droplet during arc period of short-circuiting transfer can not be maintained, free-flying transfer of droplet will occur.

Key words: gas metal arc welding; short-circuiting transfer; electromagnetic force; dynamic force equilibrium; stability

Effect of flux surface preparation on coating bonding strength LI Hui, ZHENG Lijun, WEI Qi, LI Zhuoxin (College of Material Science and Engineering, Beijing University of Technology, Beijing 100124, China). p 9—12, 16

Abstract: Flux surface preparation on ZL101 substrate was carried out to form Ni5Al coating by plasma spray. The mechanism of the coating was analyzed by calculation for interfacial temperature. The effect of process parameters on bonding strength of the coating was studied by three-factor, three-level orthogonal experiments. The results show that preplacing flux prior to spraying can substantially improve the adhesion of the coating, and the temperature of sprayed particles and the substrate temperature play determinative roles in the interfacial bonding. The optimal process parameters are the spray distance of 120 mm, the specific quantity of prelaid flux of 80 mg/cm^2 and the preheating temperature of 573 K.

Key words: plasma spray; flux surface preparation; orthogonal optimization

Effect of pitting on electrode life in spot welding hot galvanization steel with high strength ZHANG Xuqiang[1], ZHANG Yansong[2], CHEN Guanlong[2] (1. School of Mechanical Engineering, Petroleum University of China, Dongying 257061, China; 2. School of Mechanical Engineering and Power, Shanghai Jiaotong University, Shanghai 200030, China). p 13—16

Abstract: Finite element model of pitting during spot welding process was established to study the effect of pitting on temperature and stress distribution on electrode face, and corresponding experiments were carried out. The results show that higher temperature and pressure are produced at pitting area, which reduce electrode life. Micro-crack is also easily produced in pitting area at the higher temperature and pressure; through the crack, metal elements in galvanized coat are filtered into electrode, which accelerate electrode invalidation.

Key words: spot welding; hot galvanized high-strength steel; electrode life; pitting

Development of piezoelectric transducer for ultrasonic welding QI Haiqun, SHAN Xiaobiao, XIE Tao (School of Mechanical and Electrical Engineering, Harbin Institute of Technology, Harbin 150001, China). p 17—20

Abstract: In the basis of theoretical analysis, some fundamental four-terminal network matrices and frequency equations of variable cross-sectional bar on various motion state are given in order to investigate convenient and precise designing method, and a new design method of piezoelectric transducer used in ultrasonic welding is studied. The piezoelectric transducer and the variable amplitude bar are designed by four-terminal network method. The resonant characteristics are analyzed and the vibration performance is measured for the vibration apparatus with an impedance analyzer. The results show that the analysis and the design are correct.

Key words: variable cross-sectional bar; piezoelectric transducer; four-terminal network method; performance analysis

Effects of Ga, Al and Ag multi-additions on wetting properties of Sn-9Zn lead-free solders WANG Hui, XUE Songbai, CHEN Wenxue, WANG Jianxin (College of Materials Science and Technology, Nanjing University of Aeronautics and Astronautics, Nanjing 210016, China). p 21—24

Abstract: Wetting balance method is used to evaluate the effects of Ga, Al, and Ag multi-additions on the wetting property of Sn-9Zn lead-free solders. Results show that the optimal loading of Ga, Al, and Ag is 0.2 wt. %, 0.002 wt. %, and 0.25 wt. % respectively. The intermetallics formed at the interface of Sn-9Zn-0.2Ga-0.002Al-0.25Ag solder and Cu/Ni/Au substrate is investigated by scanning electron microscope (SEM) and energy dispersive spectroscopy (EDS) analysis. SEM images illustrate that two portions, a planar $AuZn_3$ layer and an additional continuous scallop-like $AuAgZn_2$ layer, formed in the intermetallics. Meanwhile, X-ray photoelectron spectroscopy (XPS) and Auger electron spectroscopy (AES) analysis on the surface components of Sn-9Zn-0.2Ga-0.002Al-0.25Ag solder indicate that Al aggregates at the surface of the solder in the form of Al_2O_3 protective film which prevents the solder from further oxidation and improves the wettability in consequence.

Key words: lead-free solder; Sn-Zn; Ga; wettability

Testing and analysis of arc shape and globule transfer of welding wire attached to 980 MPa-class steel LI Mingli[1], YANG Zhansheng[2], LI Huan[2], SUN Be[2], LIU Peng[2] (1. Mechanical Engineering School, Bejing Institute of Petrochemical Technology, Beijing 102617, China; 2. Material Science and Engineering College, Tianjin University, Tianjin 300072, China). p 25—29

Abstract: Several high-speed images of arc shape and globule transfer are obtained while using laser to be the background light of the imaging system. The arc shape and globule transfer modes of two kinds of newly researched weld wire attached to the steel with the yield intensity of 980 MPa class are studied. On condition of typical welding parameters, the MIG welding method which uses different proportions of mixture of Ar and He as protecting gases is used to conduct contrastive experiments in the arc shape and globule transfer modes between the welding wire developed and the common wire H08Mn2SiA. The results show that the weld wire is able to meet the need of mechanical capability of deposited metal, but superior in globule transfer performance to the common wire, and provides important basis for experiments of welding procedure performance of filler metals and practical applications.

Key words: 980 MPa-class steel; welding wire; arc shape; globule transfer; high-speed images

Effect of Cu addition on Sn-9Zn lead-free solder properties HUANG Huizhen, LIAO Fuping, WEI Xiuqin, ZHOU Lang (School of Materials and Engineering, Nanchang University, Nanchang 330031, China). p 30—33, 38

Abstract: Reinforced Sn-Zn-based composite solders of in-situ IMC particle were obtained by adding Cu powders into Sn-9Zn melts. The melting behavior, microstructures, mechanical properties and the wettability to Cu of the solders were studied. The results show that the effect of a small amount Cu on the melting behavior can be negligible, but 3 wt. % Cu powder addition can increase its liquidus temperature. Cu_5Zn_8 particles are formed and distributed uniformly in the solders. The coarse rod-like Zn-rich phase decreases with the addition of Cu powder. The strength and plasticity of the solder are improved, and the creep resistance of the solder is considerably enhanced. Wettability of these composite solders is also better than that of Sn-9Zn.

Key words: lead-free solder; Sn-Zn alloy; in-situ; reinforced composite; wettability

Design of stabilized high-voltage source with PWM-BUCK for electron beam welder MO Jinhai[1,2], WEI Shouqi[2], HE Shaojia[2], ZOU Yunping[1] (1. College of Electrical & Electronic Engineering, Huazhong University of Science and Technology, Wuhan 430074, China; 2. School of Mechanical and Electrical Engineering, Guilin University of Electronic Technology, Guilin 541004, China). p 34—38

Abstract: A novel PWM-BUCK type of high-voltage accelerating stabilized power source system for electron beam welder is introduced, and the switch current-limiting circuit is built to prevent surge current and over current, which increase the system reliability and stability. By means of SABER simulation, the open and closed loop characteristics of the system are analyzed in detail. A PID controller with power supply feed-forward compensation for the voltage control is proposed, and the setting principle and procedure of parameters for the controller are discussed. The simulation and application results show that this system has high control precision, good dynamic behavior, high energy conversion efficiency, low working condition requirements and high working reliability.

Key words: electron beam welder; high voltage source; pulse width modulation; switching power supply; SABER simulation

Quick-change technology of work tools for a remote welding robot CHEN Youquan[1,2], GAO Hongming[1], DONG Na[1], WU Lin[1], FAN Lidan[3] (1. State Key Laboratory of Advanced Welding